THE JOURNAL OF PHYSICAL CHEMISTRY B

Article

DFT Study of the Reaction Mechanisms of Carbon Dioxide and Its Isoelectronic Molecules CS and OCS Dissolved in Pyrrolidinium and Imidazolium Acetate Ionic Liquids

Yann Danten, Maria Isabel Cabaco, Joao A.P. Coutinho, Noel Pinaud, and Marcel Besnard

J. Phys. Chem. B, **Just Accepted Manuscript** • DOI: 10.1021/acs.jpcb.6b03229 • Publication Date (Web): 17 May 2016

ACS Publications

The Journal of Physical Chemistry B is published by the American Chemical Society. 1155 Sixteenth Street N.W., Washington, DC 20036

DFT Study of the Reaction Mechanisms of Carbon Dioxide and its Isoelectronic Molecules CS_2 and OCS Dissolved in Pyrrolidinium and Imidazolium Acetate Ionic Liquids

Y. Danten[a] *, M. I. Cabaço[b,c], J. A. P. Coutinho[d], Noël Pinaud[a] and M. Besnard[a]

[a] Institut des Sciences Moléculaires, CNRS (UMR 5255), Université Bordeaux, 351 Cours de la Libération 33405 Talence Cedex, France.

[b] Centro de Física Atómica da UL, Av. Prof. Gama Pinto 2, 1694-003 Lisboa Codex.

[c] Departamento de Física, Instituto Superior Técnico, UTL, Av. Rovisco Pais 1049-001 Lisboa, Portugal.

[d] CICECO, Departamento de Química, Universidade de Aveiro 3810-193 Aveiro, Portugal

Corresponding author: Y.DANTEN, tel +33 5 40006359, fax +33 5 4000 8402, e-mail: y.danten@ism.u-bordeaux1.fr

Abstract

The reaction mechanisms of CO_2 and its isoelectronic molecules OCS and CS_2 dissolved in *N-butyl-N-methylpyrrolidinium acetate* and in *1-butyl-3-methylimidazolium acetate* were investigated by DFT calculations in 'gas phase'. The analysis of predicted multi-step pathways allowed calculating energies of reaction and energy barriers of the processes. The major role played by the acetate anion in the degradation of the solutes CS_2 and OCS as well as in the capture of OCS and CO_2 by the imidazolium ring is highlighted. In both ionic liquids, this anion governs the conversion of CS_2 into OCS and of OCS into CO_2 through interatomic S-O exchanges between the anion and the solutes with formation of thioacetate anions. In imidazolium acetate, the selective capture of CS_2 and OCS by the imidazolium ring competes with the S-O exchanges. From the calculated values of the energy barriers a basicity scale of the anions is proposed. The ^{13}C-NMR chemical shifts of the predicted adducts were calculated and agree well with the experimental observations. It is argued that the scenario issued from the calculated pathways is shown qualitatively to be independent from the functionals and basis set used, constitute a valuable tool in the understanding of chemical reactions taking place in liquid phase.

I. Introduction

Understanding the solvation and capture of carbon dioxide (CO_2) in ionic liquids (IL) has motivated substantial applied and fundamental investigations in the field of 'green chemistry'[1-13]. In this context, imidazolium acetates constitute a class of model systems able to dissolve unusual amounts of CO_2 thus appearing as a privileged media for CO_2 capture[14-17].

Studies have shown that CO_2 spontaneously reacts with 1-butyl-3-methylimidazolium acetate [Bmim][Ac] to form imidazolium-2-carboxylate and acetic acid [14, 18-31]. This carboxylation reaction has been interpreted as due to the interaction of CO_2 with the 1-butyl-3-methylimidazole-2-ylidene (IYC) formed after the proton exchange between the acidic proton (in C_2-position) of the imidazolium cation and the acetate anion[14, 22-23, 26].

Spontaneous reactions of carbon disulfide (CS_2) or carbonyl sulfide (OCS) in imidazolium acetate solutions are also expected to form 1-butyl-3-imidazolium-2-dithioca*rboxylate* (BmimCSS) and 1-butyl-3-imidazolium-2-thiocarboxylate (BmimOCS). Such a hypothesis appears reasonable as long-lived carbenes are known to react with CS_2 [7, 32-34]. This is of particular importance because CS_2 and OCS are both involved in the global cycling of sulfur[35-39]. In particular, the OCS molecule is one of the most abundant long-lived sulfur gases trace released into the atmosphere by oceans and by anthropogenic and natural sources, constituting a strong greenhouse gas [40].

Recently, solutions of CS_2 in [Bmim][Ac] have been investigated by NMR and Raman spectroscopies [41]. Surprisingly, the formation of BmimCSS species was not detected in these solutions. In contrast, unexpected adducts, 1-butyl-3-imidazolium-2-carboxylate (BmimCOO) and thioacetate anion (CH_3COS^-) together with acetic acid in the liquid phase and CO_2 and OCS in the gaseous phase have been observed. These results showed that, besides the role played by the cation in the formation of imidazolium-carboxylate and imidazolium-thiocarboxylate species, other reactive pathways exist in which the acetate anion plays a competitive and relevant role. The coexisting reactive pathways give rise to the degradation of the solute CS_2 into OCS and CO_2 molecules through interatomic S-O exchanges between the anion and the solutes in these imidazolium-acetate solutions [41].

To achieve a better insight on the respective role of the ions in the IL, solutions of CS_2 in N-butyl-N-methylpyrrolidinium acetate [BmPyrr][Ac] have been investigated [42]. The choice of $[BmPyrr]^+$ cation, which does not form a carbene [43], allowed disentangling the role of the anion and the cation in the reactions. It was found that the acetate anions play an important role in conditioning chemical reactions with CS_2 leading to the degradation of this molecule to form thioacetate anion, CO_2, OCS, and trithiocarbonate (CS_3^{2-}) anions, via coupled complex reactions [42]. The formation of these species clearly results from the exchange of an oxygen atom of the acetate anion and a sulfur atom of either CS_2 or nascent OCS [41-42]. In marked contrast, the cation did not lead to the formation of any adducts with a role, at most, limited in assisting indirectly these reactions.

The present study is aimed at understanding the reaction mechanisms taking place in both [BmPyrr][Ac] and [Bmim][Ac] solutions with CS_2. We propose for these systems a reactive scheme including a minimal set of reactions able to predict the formation of the different adducts

experimentally observed in solution[41-42]. The analysis of the predicted 'gas phase' pathways related to each of the reaction mechanisms is modeled by Density Functional Theory (DFT) calculations using different functionals and basis sets from a system composed by a solute (CS_2 or its degradation products OCS or CO_2) interacting with a ion pair acetate-cation. The established chemical scheme allows calculating ^{13}C NMR spectral features to be compared with the experimental results. The ensemble of predictions obtained in this study concerning the chemical reactions, the formed adducts and their NMR spectra provide a consistent picture of the complex set of coupled processes taking place in these systems.

II. Methodology and Details of the Calculations

All the DFT calculations are carried out using the program Gaussian-09 [44]. The calculated PES have been achieved using the unrestricted DFT procedure increasing significantly the variational flexibility in a single-determinant method as it is described as a linear combination of α and β spin orbitals [45-46]. The DFT calculations are achieved using three distinct functionals and two basis sets: 1-the hybrid meta-GGA (Generalized Gradient Approximation) functional **wB97XD** [47] including both empirical dispersion terms and long range corrections with the 6-311+G(d,p) basis set excepted for the sulphur (S) atoms for which the MQZVP (Modified QZVP) basis set is used [48] (level wB97XD/BS1). 2- the hybrid functional **M062X** [49] (without additional energy contributions) using the 6-311+G(d,p) basis set modified for the S atoms as previously (level M062X/BS1). 3- the hybrid GGA functional **B3LYP**, known giving reliable results for investigating a large class of reactions [50-52], using the 6-31+G(d,p) basis set modified for the S atoms with the MQZVP basis set (level B3LYP/BS2). The calculations obtained with the functional wB97XD are presented here leaving the others for discussion in the SI (see also section V.1).

The multi-step 'gas-phase' pathways are evaluated from the examination of the relaxed Potential Energy Surfaces (PES) for a triatomic molecule interacting with the ion pair [BmPyrr][Ac] or the ion pair [Bmim][Ac] in a restricted domain (around an initial energy minimum) using coordinates closely involved in the reaction mechanism to map out. Due to its high dimension, the knowledge of the PES is really limited to local regions of the chemical interest. The main steps of the protocol used to localize the stationary points are the following. In a first step, the energy function is computed numerically point by point from an initial energy minimum configuration by varying a coordinate (or a set of coordinates) adequately chosen with respect to the reaction to map out. This preliminary examination allows locating roughly a transition state (TS) and a local energy minimum structure able to be connected to the initial structure (via the TS point). Then, the location of a transition state is refined to and the optimization of both minima and transition state (all the coordinates are optimized) completed using a *Synchronous Transit-Guided Quasi-Newton* (STQN) method [53-55]. After locating these stationary points (TS and both minima), the connection of the transition state with both adjacent minima is ensured by computing explicitly the reaction path using the Intrinsic Reaction Coordinate (IRC) integration method [56]. Finally, only the stationary points obtained according to this procedure

(PES analysis and IRC calculations) are retained and are fully characterized by performing a normal mode vibrational analysis.

An approach including explicitly treatment of all species participating in a series of distinct reaction mechanisms is precluded by the CPU time cost needed. For this purpose, all the reaction mechanisms are treated explicitly in our study by 3-body systems (solute + cation-anion pair). Therefore, if we consider two successive reactions, the procedure to handle the ensuing reaction may need to define another 3-body system making a connection between both successive mechanisms through an hypothetic substitution between two isolated entities at infinite separation. In that case, the substitution of one adduct by the adequate species (of thioacetate by acetate or of OCS by CS_2, for instance) corresponds with an energy deviation ΔX between both structures involved in this substitution with respect to the energy of reference of the system (Structure 1.1). It is arbitrary supposed to correspond to the difference $\Delta X = X^{\infty}_2 - X^{\infty}_1$, between the isolated species 1 and 2 at infinite separation ($X=E_0$ (total electron energy), enthalpy H^0_{298K} () or Gibbs free energy G^0_{298K} at 298K) and the calculated X-values are provided in Table S1. The ΔX-energy deviations are only used for the energy diagrams shown in Figures 1-4 in order to make a connection between two successive reaction mechanisms for a given system (either [BmPyrr][Ac] $+CS_2$ or [Bmim][Ac] $+CS_2$). The ΔX-values do not intervene in the evaluation of the energy barriers and other energy observables (enthalpy of reaction, Gibbs free energy) reported in Tables S2-8 of the Supporting Information and discussed in the text.

Notice that the energy diagrams include explicitly the ZPE energy contributions and are shown with respect to the energy $E_{0+ZPE}^{(ref)}$ of the initial structure of the [BmPyrr][Ac]-CS_2 or [Bmim][Ac]-CS_2 systems, taken as the energy of reference.

Finally, the ^{13}C NMR chemical shifts are evaluated for species in the calculated initial (interacting reactants) and final structures (interacting adducts in products, Prd) using the Multi-standard Approach (MSA) with the GIAO (Gauge-Independent Atomic Orbital). This method is indeed known to provide better predictions compared to experimental chemical shifts [57].

III. Conversion of CS_2 into CO_2 in [BmPyrr][Ac]

The conversion of CS_2 into CO_2 in [BmPyrr][Ac] mainly relies on a mechanism in two successive steps through interatomic S-O exchanges. A first one between a S atom of CS_2 and an O atom of CH_3COO^- yields to OCS and CH_3COS^- adducts (Eq.1a, Scheme 1). The OCS released performs in turn a similar exchange with a surrounding CH_3COO^- to form CH_3COS^- anion and CO_2, degassing in the gas phase [42] (Eq.1b). The formation of CO_2 determines the ending of the degradation cycle of CS_2 in [BmPyrr][Ac].

[**Scheme 1**]

The existence of secondary channels of reaction involving S-O exchanges between the solutes CS_2 or OCS and CH_3COS^- ([BmPyrr] [CH_3COS^-]-CS_2 and [BmPyrr][[CH_3COS^-]-OCS systems, respectively) has been investigated. These two additional mechanisms in the degradation cycle of CS_2 (Eqs.1c, 1d,

respectively, Scheme 1) constitute further sources of OCS and CO_2 with formation of dithioacetate species ($CH_3CS_2^-$). Then, the molecule OCS can be again introduced in the degradation cycle (Eq.1b) leading to CO_2 formation.

III.1. Primary Conversion Mechanisms of CS_2 into CO_2

The analysis of the calculated PES allows evaluating a three-step reactive pathway for the conversion of CS_2 into OCS (Eq.1a). The calculated values of E^0, H^0_{298K} and G^0_{298K} for the stationary points (transition states and energy-minima, reactants, intermediates and products) along the predicted pathway are reported in the Supporting Information Table S2. The corresponding E_{0+ZPE}-energy diagram together with a schematic representation of the calculated structures are displayed in Fig. 1[1]. The detailed description of the predicted pathway is provided in the Supporting Information.

Two main steps can be distinguished and are 1) the reduction of CS_2 by acetate and 2) the interatomic S-O exchange between them. These processes demand to cross the main energy barriers (15.8 and 14.6 kcal/mol for TS1.1 and TS2.1, respectively). The final step concerns the dissociation of the CH_3COS-OCS^- intermediate anion (Int2.1) leading to the formation of OCS with CH_3COS^- adducts interacting with the [BmPyrr] cation in the final stable structure Prd1.1. Finally, the energy $\delta E^r = E_0(\text{Prd1.1}) - E_0^{(ref)}$, the enthalpy δH^r_{298K} and the Gibbs free energy δG^r_{298K} in 'gas phase' of this reaction are evaluated at -7.5, about -7.5 and -9.0 kcal/mol, respectively (Table S2). These values show that the conversion of CS_2 into OCS is an exothermic process for which a minimal amount of energy of about 16.0 kcal/mol is requested to cross the successive energy barriers.

Both adducts OCS and CH_3COS^- issued from the conversion of CS_2 into OCS (Prd1.1) can be reintroduced in the degradation cycle of CS_2. Three possible channels of reactions involving interatomic S-O exchange can be considered. Firstly, between OCS and CH_3COO^- (Eq. 1b), then between CS_2 and CH_3COS^- (Eq. 1c) and finally involving now the formed CH_3COS^- (Eq. 1d). Notice that these two latter channels are conditioned by the population of CH_3COS^-. Thus, at low concentrations of CS_2 in the IL, the conversion of OCS into CO_2 involving CH_3COO^- appears statistically more probable than the same process with CH_3COS^-. For this reason, the S-O exchanges involving CH_3COS^- (Eqs. 1c, 1d) and leading to the formation of dithioacetate anion are considered as secondary reaction mechanisms.

The analysis of the calculated PES allows determining for the conversion of OCS into CO_2 a two-step pathway from the initial structure 1.2 (Fig. 1) which concerns again the conversion of OCS by CH_3COO^- (9.6 kcal/mol, TS1.2) followed by the S-O exchange between them (15.5 kcal/mol, TS2.2). The values of δE^r , δH^r_{298K} and δG^r_{298K} are evaluated at -6.3, -6.2 and -6.7 kcal/mol, respectively.

[1] In the E_{0+ZPE}-energy diagrams displayed in Figure 1, we applied the adequate translations in the calculated energies ΔX ([BmPyrr][CH_3COO^-]-OCS) and ([BmPyrr][CH_3COS^-]-CS_2) (with $X=E^0$, H^0_{298K}, G^0_{298K}, see discussion in section II) related to the replacement from the structure Prd1.1 (end point of Eq.1a) of thioacetate (removed at the infinite) by acetate (coming from the infinite) in the structure 1.2

Globally, the conversion of CS_2 into CO_2 results from two successive exothermic mechanisms favoured in 'gas phase' even if about 16.0 kcal/mol are needed to cross the energy barriers.

III.2. Secondary conversion of CS_2 and OCS with thio-acetate

The analysis of the calculated PES shows that the secondary conversions of CS_2 and OCS with thioacetate are three-step pathways as shown in E_{0+ZPE}-energy diagrams (Fig.2, Eqs. 1c, 1d, Scheme 1). The initial structures (1.3 and 1.4) involve CS_2 and OCS, respectively. Both secondary conversions exhibit similar features to those involving acetate (Fig.2, Eqs. 1a, 1b). However, the energy barriers (TS1 and TS2) are significantly higher than those evaluated for the same mechanisms with acetate (displayed in Fig 2 for comparison) and the final structures Prd1.3 and Prd1.4 are comparatively less stable (see Supporting Information in Tables S2 and S3). In addition, the energies of reaction δE^r are calculated with higher values about -2.9 and -6.5 kcal/mol, respectively. Thus, the interatomic S-O exchanges between the solutes CS_2 or OCS and thioacetate are always exothermic processes but having higher energy barriers (> 18.0 kcal/mol). The activation of these secondary mechanisms is disfavoured due to the existence of higher energy barriers. Therefore the activity of such secondary reaction can be revealed by the presence of the species dithioacetate.

III.3. ^{13}C NMR spectral signatures

The calculated ^{13}C NMR chemical shifts of the reactants and products are compared with the corresponding chemical shifts of resonance lines experimentally observed in [BmPyrr][Ac]-CS_2 solutions [42] (Table 1). This comparison show that fairly good agreement exists for the CH_3COS^-, CO_2 and OCS adducts. These spectral signatures provide evidence for the existence of the conversion processes of CS_2 into OCS and OCS into CO_2 in solution. The absence of the ^{13}C resonance line of CS_2 (reported at 193 ppm in the literature [58] and evaluated at 195 ppm in this work) suggests that this solute is fully consumed by the degradation processes at the concentrations investigated experimentally. The absence of the resonance line assigned to the $-CS_2^-$ group of $CH_3CS_2^-$(expected at 263 ppm) clearly indicates that the S-O exchange process between thioacetate and CS_2 or OCS is inoperative in these solutions [42]. This finding results from the lower basicity of thioacetate compared to that of acetate which leads to higher energy barriers crossing for the reduction of both solutes (see section V.2). Finally, we conclude that the exothermic conversion of CS_2 into CO_2 by successive interatomic S-O exchanges between the CS_2 and OCS with acetate is clearly put in evidence by ^{13}C NMR spectral signatures. In contrast, the secondary interatomic S-O exchanges between CS_2 and OCS with thioacetate, which are also predicted as being exothermic processes, are inactive as proved by the absence of the NMR spectral signature of the dithioacetate anion.

IV. Conversion and Capture of CS_2 in [Bmim][Ac]

In [Bmim][Ac] the conversion of CS_2 into OCS and OCS into CO_2 and the capture of CS_2 and its degradation adducts (OCS and CO_2) by the [Bmim] cation coexist. Firstly, five primary competitive

channels (Scheme 2) are considered. Three of them concern the capture of a solute (CS_2, OCS or CO_2) by the imidazolium ring leading to the formation of imidazolium carboxylate species (BmimCSS, BmimOCS and BmimCOO, Eqs. 2a, 3a and 4, respectively). The two other reactive channels concern the conversion of CS_2 into OCS (Eq. 2b) and of OCS into CO_2 (Eq. 3b) with the formation of CH_3COS^-. Then, additional secondary channels of reactions involving the formed thioacetate in S-O exchanges and capture processes of the solutes by the cation are considered (Eq. 5a, 5b, 6a, 6b).

[**Scheme 2**]

IV.1. Primary channels of reactions

The predicted pathways related to the five main processes of the reaction scheme have been determined to evaluate the energy barriers and the energies of reaction (Scheme 2). The analysis of the calculated PES for the [Bmim][Ac]-CS_2 system allows determining two pathways (Eqs. 2a and 2b) from an initial structure 1.1 (Fig. 3). A detailed description of the pathways with a schematic structural representation of the calculated stationary points is provided in the Supporting Information. The calculated E_{0+ZPE}-energy diagram (at the wB97xD/BS1 level) is displayed in Fig. 3A and the calculated energy values are gathered in the Supporting Information, Table S5.

The capture of CS_2 by the [Bmim] cation (Eq. 2a) involves two well-defined steps which are the exchange of the acidic proton (at the C_2 position) of the cation with acetate and the insertion of CS_2 in the imidazolium ring to form imidazolium dithiocarboxylate (BmimCSS). The deprotonation of the cation gives rise to a first intermediate (Int1.1) in which CS_2 specifically interacts with the couple *acetic acid–1-butyl-3-methyl-imidazole-2-ylidene-carbene* (IYC) triggering the selective insertion of CS_2 in the IYC ring. The reduction of CS_2 by IYC with an energy barrier (TS2.1) of about 24.7 kcal/mol yields to the insertion of the solute in the IYC ring to form BmimCSS with production of acetic acid (Prd1.1, Fig. 3 and Table S5).

The conversion of CS_2 into OCS constitutes a competitive channel to the dithio-carboxylation reaction. The interatomic S-O exchange between acetate and CS_2 is described by a three-step pathway (Eq. 2b) from the initial structure 1.1 (Fig. 3 and Table S5). The successive steps are similar to those described for the [BmPyrr] cation (section III). Firstly, CS_2 is reduced by acetate to form after the crossing of a first energy barrier (TS1.2, about 18.0 kcal/mol), a first intermediate anion $CH_3COO\text{-}CS_2^-$ (Structure Int1.2), followed by the S-O exchange with a second energy barrier (TS2.2) yielding to a second intermediate anion $CH_3COS\text{-}OCS^-$ (Int2.2). Finally this structure is dissociated into CH_3COS^- and OCS in interaction with the [Bmim] cation (Prd 1.2).

The energy of reaction δE^r of the CS_2 capture is evaluated at -13.5 kcal/mol whereas it is -5.3 kcal/mol for the conversion of CS_2 into OCS (δH^r_{298K} and δG^r_{298K} values in Table S5). However, the capture of CS_2 by the imidazolium ring needs to cross a higher energy barrier (about 24.7 kcal/mol) to proceed to the reduction of CS_2 by IYC whereas the successive energy barriers related to the conversion of CS_2 into OCS are significantly lower (about 18 kcal/mol, Fig. 3). Moreover, the formation of OCS does not constitute the breaking of the degradation cycle of CS_2 as it was previously shown for solutions of CS_2

in [BmPyrr][Ac]. Additional channels of reactions related to the capture of OCS by the [Bmim] cation (Eq. 3a) and the conversion of the formed OCS into CO_2 (Eq. 3b) through two steps pathways have been determined (Fig. 3, detailed discussion provided in the Supporting Information). The capture of OCS by the imidazolium ring results from two successive steps similar to those found for CS_2, deprotonation (at the C_2 position) of the [Bmim] cation followed by the reduction of OCS by the IYC species and the insertion in ~~of~~ the IYC ring. The values of the energy barriers (TS1.3 and TS2.3) associated with these mechanisms are about 3.3 and 18.3 kcal/mol, respectively (Table S5).

The conversion of OCS into CO_2 (Eq. 3b) involves the reduction of OCS by acetate (TS1.4, about 10.9 kcal/mol) followed by the interatomic S-O exchange (TS2.4, about 20.5 kcal/mol) to form CH_3COS^- and CO_2 adducts interacting with the cation (Fig. 3). The calculated energy barriers of capture and conversion of OCS are quite comparable. These reactions are exothermic processes with energy of reaction δE^r evaluated at -4.6 and -2.2 kcal/mol, respectively (Table S5) [2].

Finally, the formed CO_2 is captured by the [Bmim] cation (Eq. 4), leading to the formation of the imidazolium carboxylate. Again, the process is described by a two-step pathway related to the proton exchange between the acetate-imidazolium ion pair (TS1.5 about 4.9 kcal/mol) to form the couple acetic acid–IYC (structure Int1.5) followed by the reduction of CO_2 by IYC (TS2.5 about 14.7 kcal/mol) and its insertion in the IYC ring. This carboxylation is characterized by an energy of reaction about -3.9 kcal/mol close to that evaluated in a previous study [59] (Table S5). The δH^r_{298K} and δG^r_{298K} values are evaluated at -4.6 and -1.0 kcal/mol, respectively.

IV.2. Secondary channels of reactions

These channels are associated with the capture of the CS_2 and OCS molecules by the imidazolium ring in presence of thioacetate (Eqs. 5a, 6a, Scheme 2) and the S-O exchanges between thioacetate and CS_2 and OCS (Eqs. 5b, 6b). The calculated values of the E_{0+ZPE} energy are displayed in Fig.4 and compared to those of the main reactions previously discussed. It appears that the conversion processes of CS_2 into OCS (Eq. 5b) and of OCS into CO_2 (Eq. 6b) are quite similar to the corresponding mechanisms with acetate (Eqs.2b and 3b). They are characterized by two main energy barriers successively due to the reduction of the solute and the S-O exchange. For CS_2 solute the corresponding values are about 21.2 (TS1.6) and 21.2 kcal/mol (TS2.6) and for OCS solute 15.8 (TS1.7) and 24.3 kcal/mol (TS2.7). In presence of thioacetate anion the values of energy barriers are slightly higher than those involving the same solute with the acetate anion. Indeed, the corresponding values involving acetate and CS_2 are 18.0 and 17.0 (conversion and exchange) whereas they are 10.9 and 20.6 kcal/mol for OCS solute (Fig. 3, cf. Tables S5-6).

[2] It comes out that if the energy fluctuations allow activating the conversion process of OCS into CO_2, they also activate the channel of reaction related to the thio carboxylation in the same time. In that case, both mechanisms could coexist in the CS_2/[Bmim][Ac] solutions.

The capture of CS_2 and OCS by IYC in presence of thioacetate (Eqs.5a, 6a) are one-step reaction mechanisms in contrast with the same reactions in presence of acetate which involve two-steps. Therefore, the proton exchange between the [Bmim] cation and the thioacetate anion followed by the reduction of the solute by IYC are processes more intimately coupled (Fig. 4). The values of height of the barriers associated to this capture follow the hierarchy found for the higher barrier in acetate according to ~ 22 kcal/mol(CO_2) < 25 kcal/mol(OCS) < ~33 kcal/mol(CS_2). It is noteworthy that in presence of thioacetate the capture of OCS and CO_2 by the imidazolium ring are endothermic processes (δE^r about +3.1 and +2.4 kcal/mol, respectively) whereas the capture of CS_2 is an exothermic reaction. On the ground of the reaction energy criteria, only the capture of CS_2 by IYC in presence of thioacetate is allowed. However, this mechanism involves higher energy barrier than that existing in presence of acetate anion (33 vs. 25 kcal/mol, respectively).

IV.3 ^{13}C NMR spectral signatures

The calculated ^{13}C NMR chemical shifts of the reactants and products are compared with experimental values of the species detected in solutions in Table 2. The calculated chemical shifts of the species formed in the conversion processes are very close to those found in the [BmPyrr][Ac]-CS_2 system. The differences between the two sets of values are very small and can be ascribed to the effect of the different environments (Tables 1 and 2). The agreement with experimental results provides again compelling evidence for the existence of the proposed conversion processes of CS_2 into OCS and OCS into CO_2.

The capture processes leading to the formation of BmimCOS and BmimCOO are confirmed by the ^{13}C resonance lines of the groups COS and COO of these imidazolium carboxylate species (evaluated at about 183-203 and 146 ppm, and detected at 192 and 155 ppm, respectively). This is also confirmed by the spectral lines assigned to the C_2-atom of those species (evaluated at about 150 and 140 ppm and detected at 145 and 142 ppm, respectively) (Table 2). In marked contrast, the formation of the BmimCSS was not observed as testified by the absence of the ^{13}C resonance line of the CSS group of this species (expected at 226-229 ppm [6, 34, 60] and calculated at 227-228 ppm). Clearly, the conversion of CS_2 into OCS is favoured in solution compared to the CS_2 capture by the imidazolium ring, as suggested by DFT results. This can be understood as due to the higher energy barrier involved in the reduction of CS_2 by IYC. The absence of well-defined resonance lines due to BmimCSS, dithioacetate and thioacetic acid (expected at 228, 263 and 218 ppm, respectively) allow disregarding the reaction pathways involving the thioacetate anion as reactant in the domain of concentration experimentally investigated (Eqs. 2a and 5a). These reaction processes involve higher energy barriers than those obtained when acetate anion is concerned. The highest energy barriers involving thioacetate encountered along each of the reaction pathways related to the exchange and the capture processes are evaluated in the range 21 to 33 kcal/mol (Fig. 4). The smallest value is related to the interatomic S-O exchange between thioacetate and CS_2 to form dithioacetate anion (Eq. 5b). However, the absence of spectral features for this species in solution indicates that the mean amplitude of the energy

fluctuations available is likely lower than 21 kcal/mol. Thus, any reaction process involving a higher energy barrier is rather inaccessible and can be definitively disregarded in these solutions. This also applies to the reduction of CS_2 by the IYC ring in solutions of CS_2 in [Bmim][Ac] (Eq. 2a).

V. Discussion of the Results

V.1. Hybrid functional and Basis set Effects

The effects on the calculated pathways of the choice of the hybrid functionals M062X and B3LYP with the BS1 and BS2 basis set have been assessed. Their E_{0+ZPE}-energy diagrams reported in the Supporting Information (Fig. S4-6 and Tables S2-8) show qualitatively similar results to those obtained at the wB97xD/BS1 level. In particular, the trends of the heights of energy barriers associated to the capture of the solutes compared to those involving the conversion processes follow the same hierarchy. Systematic deviation on the energy barriers with slightly higher values using the functional B3LYP with BS2 basis set are observed, whereas the energy of the exothermic reactions present smaller values. In contrast, using the hybrid functionals wB97xD and M062X with the BS1 basis, the results obtained remain relatively comparable. In particular, the conversion of OCS into CO_2 and the reduction of OCS by the IYC ring have comparable predicted energy barriers (for a given model, cf. Fig.4 and Fig. S 6-8). This suggests that both mechanisms coexist as attested by the observed NMR spectral signatures of BmimOCS and BmimCOO species in solution (cf. & IV.3). Globally, the scenario coming out from the energetic criteria is not qualitatively affected by the choice of the functionals and basis set.

V.2. Influence of the anion Basicity

The analysis of the energy profiles (E_{0+ZPE}-energy diagrams, Fig. 1-4) in solutions of CS_2 in [BmPyrr][Ac] and [Bmim][Ac] shows that the conversion of CS_2 into CO_2 by S-O exchanges between acetate and the CS_2 and OCS solutes are reactive channels particularly efficient. This result shows that the anions (acetate and its thio-derivatives) play a central role in the reactions mechanisms which can be rationalized on the ground of their basicity. The basicity is usually defined in 'gas phase' as the negative Gibbs free-energy change related to the reaction: $A_{(g)}^- + H_{(g)}^+ \rightarrow AH_{(g)}$ where the anion A^- is the conjugate base associated with the neutral acid AH. The most accurate gas phase basicity (GPB) values are obtained using the CBS-QB3 method [61]. For the acetate anion, we have evaluated the GPB using this method at about 339.4 kcal/mol, close to the experimental value (341.4 ± 1.2 kcal/mol [62]. The GPB-values of thio- and dithioacetate anions have been evaluated with the same approach to be 324.8 and 322.4 kcal/mol, respectively. Considering these values the basicity for acetate anions and its thio-derivatives is found to follow the hierarchy: $[CH_3CS_2] < [CH_3COS] < [CH_3COO]$ [3]. This shows

[3] Incidentally, the GPB of the trifluoroacetate anion (CF_3COO^-) is evaluated at 315.5 kcal/mol. This results from the electron withdrawing effect due to fluorine atoms and localizes this anion at the lowest GPB value of the acetate anion scale above. Notice that there is no reaction by dissolution of CO_2 in [Bmim][CF_3COO]. [63]

that for the thio-derivatives of the acetate anion the substitution of an oxygen by a sulfur atom leads to a decreasing of basicity. In the context of the present study, such an approach considering an acid and its conjugate base does not appear appropriate to describe such complex systems. Hence, we still keep the height of energy barriers associated with the reduction of the solute as a criterion for the definition of the anion basicity, but now for the reactions in the systems considered here (differing from the proton transfer reaction taken as a standard to define GBP). The examination of the calculated values of the energy barriers for the acetate anion and its thio-derivatives leads to the scale $[CH_3CS_2] < [CH_3COS] < [CH_3COO]$. Thus, the lower is the barrier, the higher the basicity of the anion. It is noteworthy that such a hierarchy is the same as that found for the GBP values discussed before.

Incidentally, in the interatomic exchange processes discussed here, the nature of the pyrrolidinium or imidazolium cations have rather little influence on energy barriers and at most assist the reactions via the polarity of the medium.

For the capture of CS_2, OCS and CO_2 by the IYC ring in [Bmim][Ac], although the anions do not explicitly participate to the reduction of the solute, the values of the energy barriers are greater in the case of thioacetate (33, 25 and 21 kcal/mol, respectively) than those for acetate anions (25, 18 and 15 kcal/mol, respectively). This result shows that it exists an implicit influence of the anion in the capture processes, even if, the energy barriers due to the reduction of the solute by the IYC ring follow mainly the hierarchy according to : $(CO_2) < (OCS) < (CS_2)$, as previously mentioned.

VI. Conclusion

The main objective of this study was to clarify the role played by the acetate anion in solutions of CS_2 in [BmPyrr][Ac] and in [Bmim][Ac]. The reactions occurring in solution have been assessed using DFT calculations from a minimal set of primary and secondary reaction mechanisms in 'gas phase' on the ground of energetic criteria (energy barriers and energies of reaction). The analysis of the calculated reaction profiles shows that preliminary reduction of the solute by acetate followed by the solute-anion interatomic S-O exchanges are processes found in both solutions.

In [BmPyrr][Ac]-CS_2 solutions, only the conversion of CS_2 into OCS and of OCS into CO_2 by the acetate anion coexist (primary reaction mechanisms). The conversion mechanisms involving the formed thioacetate anion having higher activation energy for the reduction of a solute are inoperative, hence supporting the non observation of dithioacetate species by RMN (secondary mechanisms).

In [Bmim][Ac] solutions, the conversion processes of CS_2 into OCS and of OCS into CO_2 coexist with the selective insertion of OCS or CO_2 adducts in the imidazolium ring. The existence of a proton exchange between acetate and the cation allows a specific interaction of the solute with a 'transient' neutral IYC species to form a solute-IYC complex in presence of acetic acid (primary mechanism). The selective insertion of the solute in the imidazolium ring depends on the height of the energy barrier associated to the reduction of the solute by IYC. The absence of imidazolium dithiocarboxylate species (BmimCSS) in solution is rationalized by the DFT calculations. Indeed, the energy barriers

corresponding to the conversion of CS_2 by acetate and to the interatomic S-O exchange between them are significantly lower than those associated to the reduction of CS_2 by IYC. Concomitantly, the absence of $CH_3CS_2^-$ species is interpreted as a consequence of the higher activation energy in presence of thioacetate as found previously for [BmPyrr][Ac]-CS_2. This result allows ruling out any S-O exchanges involving thioacetate in solutions investigated here.

The examination of the calculated values of the energy barriers for the reduction of a solute by the acetate anion and its thio-derivatives led to the basicity scale $[CH_3CS_2]$ < $[CH_3COS]$ < $[CH_3COO]$. This scale is consistent with that derived from the proton capture by an anion in gas phase. The approach used here is more appropriate to discuss specifically the complex and coupled reactions described in this study, which are far away from a single proton transfer between an acid and its conjugate base.

The main result of this study is that 'gas phase' modeling using DFT calculations based on a minimal set of distinct mechanisms allow to quantitatively predict the reactions and the coexisting adducts in solutions of CS_2 in [BmPyrr][Ac] and [Bmim][Ac]. It allows provides an explanation for the absence of the BmimCSS adduct in [Bmim][Ac]-CS_2 and of $CH_3CS_2^-$ anion in both solutions. A further relevant issue is that using the MSA approach, the predicted ^{13}C NMR spectra with chemical shifts are in good agreement with the experimental results.

The ensemble of 'gas phase' predictions concerning the chemical reactions leads to a scenario qualitatively consistent with the interpretation of the experimental results (adducts observed by NMR spectra) independently of the functionals and basis set used in the DFT calculations. This study shows that these calculations having in principle their application domain in gas phase, do constitute a valuable tool in the understanding of chemical reactions in liquid phase. These results are encouraging for further studies relevant to this domain.

SUPPORTING INFORMATION AVAILABLE

Calculated Energies (total electron energy E^0, enthalpy $H°_{298K}$ and Gibbs free $G°_{298K}$ energies at 298K (including the Zero Point Energy (ZPE) contribution) of the stationary points along the different predicted pathways of the reaction schemes I and II (Tables S2-8). Detailed descriptions of the predicted reaction paths. Hybrid functional and basis set effects. Schematic representation of the (stationary points) structures along the different calculated pathways (Figures S1-7).

ACKNOWLEDGEMENTS

This work was partly developed in the scope of the project CICECO-Aveiro Institute of Materials (Ref. FCT UID/CTM/50011/2013), financed by national funds through the FCT/MEC and when applicable co-financed by FEDER under the PT2020 Partnership Agreement. The authors gratefully acknowledge the support provided by the M3PEC computer centre of the DRIMM (Direction des

resources Informatiques et Multimédia Mutualisée, Talence, France) of the New University of Bordeaux and the IDRIS computer centre of the CNRS (Institut du Développement et des Resources en Informatique Scientifique, Orsay, France) for allocating computing time and providing facilities.

REFERENCES

1. Rogers, R. D.; Seddon, K. R., *Ionic Liquids as Green Solvents. Progress and Prospects*. ACS Symposium Series: Washington, 2003; Vol. 856, p 2-12.
2. Cadena, C.; Anthony, J. L.; Shah, J. K.; Morrow, T. I.; Brennecke, J. F.; Maginn, E. J., Why Is CO2 So Soluble in Imidazolium-Based Ionic Liquids? *J. Am. Chem. Soc.* **2004,** *126* (16), 5300-5308.
3. Castner, E. W.; Wishart, J. F., Spotlight on Ionic Liquids *J. Chem. Phys.* **2010,** *132*, 12091.
4. Castner , E. W.; Wishart, J. F.; Shirota, H., Intermolecular Dynamics, Interactions and Solvation in Ionic Liquids. *Acc. Chem. Res.* **2007,** *40* (11), 1217-1227.
5. Wishart, J. F.; Castner, E. W., The Physical Chemistry of Ionic Liquids. *J. Phys. Chem. B* **2007,** *111* (18), 4639-4640.
6. Delaude, L., Betaine Adducts of N-Heterocyclic Carbenes: Synthesis, Properties, and Reactivity. *Eur. J. Inorg. Chem.* **2009,** (13), 1681-1699.
7. Delaude, L.; Demonceau, A.; Wouters, J., Assessing the Potential of Zwitterionic NHC·CS2 Adducts for Probing the Stereoelectronic Parameters of N-Heterocyclic Carbenes. *Eur. J. Inorg. Chem.* **2009,** (13), 1882-1891.
8. Maginn, E. J., Molecular Simulation of Ionic Liquids: Current Status and Future Opportunities. *J. Phys.: Condens. Matter* **2009,** *21*, 373101.
9. Brennecke, J. F.; Gurkan, B. E., Ionic Liquids for CO2 Capture and Emission Reduction. *J. Phys. Chem. Lett.* **2010,** *1* (24), 3459-3464.
10. Jutz, F.; Andanson, J. M.; Baiker, A., Ionic Liquids and Dense Carbon Dioxide : A Beneficial Biphasic System for Catalysis. *Chem. Rev.* **2011,** *111*, 322-353.
11. Zhang, J.; Sun, J.; Zhang, X.; Zhao, Y.; Zhang, S., The Recent dDevelopment of CO2 Fixation and Conversion by Ionic Liquid. *Greenhouse Gas Sci Technol.* **2011,** *1*, 142-159.
12. Zhang, Y.; Wu, Z.; Chen, S.; Yu, P.; Luo, Y., CO2 Capture by Imidazolate-Based Ionic Liquids: Effect of Functionalized Cation and Dication. *Ind. Eng. Chem. Res.* **2013,** *52* (18), 6069-6075.
13. Stevanovic, S.; Podgorsek, A.; Moura, L.; Santini, C. C.; Padua, A. A.; Costa Gomes, M. F., Absorption of Carbon Dioxide by Ionic Liquids with Carboxylates Anions. *Int. J. Grenhouse Gas Control* **2013,** *17*, 78-88.
14. Shiflett, M. B.; Kasprzak, D. J.; Junk, C. P.; Yokozeki, A., Phase Behavior of {Carbon Dioxide + [bmim][Ac]} Mixtures. *J. Chem. Thermodynamics* **2008,** *40* (1), 25-31.
15. Shiflett, M. B.; Yokozeki, A., Phase Behavior of Carbon Dioxide in Ionic Liquids: [emim][Acetate], [emim][Trifluoroacetate], and [emim][Acetate] + [emim][Trifluoroacetate] Mixtures. *J. Chem. Eng. Data* **2009,** *54* (1), 108-114.
16. Carvalho, P. J.; Alvarez, V. H.; Machado, J. J. B.; Pauly, J.; Daridon, J.-L.; Marrucho, I. M.; Aznar, M.; Coutinho, J. A. P., High Pressure Phase Behavior of Carbon Dioxide in 1-alkyl-3-methylimidazolium bis(trifluoromethylsulfonyl)imide Ionic Liquids. *J. Supercritical Fluids* **2009,** *48* (2), 99-107.
17. Carvalho, P. J.; Alvarez, V. H.; Schröder, B.; Gil, A. M.; Marrucho, I. M.; Aznar, M.; Santos, L. M. N. B. F.; Coutinho, J. A. P., Specific Solvation Interactions of CO2 on Acetate and trifluoroacetate imidazolium BasedIonic Liquids at High Pressures. *J. Phys. Chem. B* **2009,** *113* (19), 6803-6812.
18. Besnard, M.; Cabaço, M. I.; Chavez, F. V.; Pinaud, N.; Sebastião, P. J.; Coutinho, J. A. P.; Mascetti, J.; Danten, Y., CO2 in 1-Butyl-3-methylimidazolium Acetate. 2. NMR Investigation of Chemical Reactions. *J. Phys. Chem. A* **2012,** *116* (20), 4890-4901.
19. Besnard, M.; Cabaço, M. I.; Vaca-Chávez, F.; Pinaud, N.; Sebastião, P. J.; Coutinho, J. A. P.; Danten, Y., On the Spontaneous cCarboxylation of 1-butyl-3-methylimidazolium Acetate by Carbon Dioxide. *Chem. Commun.* **2012,** *48* (9), 1245-1247.

20. Cabaço, M. I.; Besnard, M.; Danten, Y.; Coutinho, J. A. P., CO2 in 1-butyil-3-imidazolium acetate: I Unusual Solubility Investigated by Raman Spectroscopy and DFT Calculations. *J Phys Chem A* **2012,** *116*, 1605-1620.
21. Carvalho, P. J.; Coutinho, J. A. P., On the Non Ideality of CO2 Solutions in Ionic Liquids and Other Low Volatile Solvents. |*J. Phys. Chem. Lett.* **2010,** *1*, 774-780.
22. Maginn, E. J., Design and Evaluation of Ionic Liquids as Novel CO2 Absorbents. In *Quaterly Technical Report to DOE*, 2005.
23. Gurau, G.; Rodriguez, H.; Kelley, S. P.; Janiczek, P.; Kalb, R. S.; Rogers, R. D., Demonstration of Chemisorption of Carbon Dioxide in 1,3-dialkylimiazolium acetate ionic liquids. *Angew Chem Int Ed* **2011,** *50* (50), 12024 –12026.
24. Holbrey, J. D.; Reichert, W. M.; Tkatchenko, I.; Bouajila, E.; Walter, O.; Tommasi, I.; Rogers, R. D., 1,3-dimethyl-imidazolium-2-carboxylate:The Unexpected Synthesis of an Ionic Liquid Precursor and carbene-CO2 Adduct. *Chem Comm* **2003**, 28-29.
25. Kelemen, Z.; Hollóczki, O.; Nagy, J.; Nyulászi, L., An Organocatalytic Ionic Liquid. *Org. Biomol. Chem.* **2011,** *9*, 5362-5364.
26. Rodriguez, H.; Gurau, G.; Holbrey, J. D.; Rogers, R. D., Reaction of Elemental Chalcogens with Imidazolium Acetates to Yield imidazole-2-chalcogenones: Direct eEvidence for IL as Proto-carbenes. *Chem. Commun.* **2011,** *47*, 3222-3224.
27. Kelemen, Z.; Peter-Szabo, B.; Székely, E.; Holloczki, O.; Firaha, D. S.; Kirchner, B.; Nagy, J.; Nyulaszi, L., An Abnormal N-Heterocyclic Carbene–Carbon Dioxide Adduct from Imidazolium Acetate Ionic Liquids: The Importance of Basicity. *Chem. Eur. J.* **2014,** *20*, 13002-13008.
28. Holloczki, O.; Gerhard, D.; Massone, K.; Szarvas, L.; Nemeth, B.; Veszpremi, T.; Nyulaszi, L., Carbenes in Ionic Liquids. *New J Chem* **2010,** *34*, 3004-3009.
29. Holloczki, O.; Kelemen, Z.; Konczol, L.; Szieberth, D.; Nyulaszi, L.; Stark, A.; Kirchner, B., Significant Cation Effects in Carbon Dioxide-ionic Liquid Systems. *Chem. Phys. Chem.* **2013,** *14*, 315-320.
30. Ken-ichi Saitow, H. O., Nobuhiko Sarukura and Keiko Nishikawa, Terahertz Absorption Spectra of Supercritical CHF3 to Investigate Local Structure Through Rotational and Hindered Rotational Motions. *Chem. Phys. lett* **2001,** *341* (1-2), 86-92.
31. Stevanovic, S.; Podgorsek, A.; Padua, A. A. H.; Gomes, M. F. C., Effect of Water on the Carbon Dioxide Absorption by 1-Alkyl-3-methylimidazolium Acetate Ionic Liquids. *J. Phys. Chem B* **2012,** *116*, 14416-14425.
32. Kuhn, N.; Steimann, M.; Weyers, G., Synthesis and Properties of 1,3-diisopropyl-4,5-dimethylimidazolium-2-carboxylate.A Stable Carbene Adduct of Carbon Dioxide. *Z Naturforsch* **1999,** *54b*, 427-433.
33. Nakayama, J.; Kitahara, T.; Sujihara, Y.; Sakamoto, A.; Ishii, A., Isolable, Stable, diselenocarboxylate and selenothiocarboxyate Salts: Synthesis, Structures, and Reactivities of 2-(1,3-dimethylimidazolidinio)diselenocarboxylate and 2-(1,3-dimethylimidazolidinio)selenothiocarboxylate. *J. Am. Chem. Soc.* **2000,** *122* (38), 9120-9126.
34. Siemeling, U.; Memczak, H.; Bruhn, C.; Vogel, F.; Trager, F.; Baio, J. E.; Weidner, Y., Zwitterionic Dithiocarbxylates Derived from N-heterocyclic Carbenes: Coordination to Gold Surfaces. *Dalton Trans.* **2012,** *41*, 2986-2994.
35. Chin, M.; Davis, D. D., Global Sources and Sinks of OCS and CS2 and Their Distributions. *Global Biogeochemical Cycles* **1993,** *7* (2), 321-337.
36. Hiraoka, K.; Fujita, K.; Ishida, M.; Nakagawa, F.; Wada, A.; Yamabe, S.; Tsuchida, T., Thermochemical Stabilities and Structures of the Cluster Ions OCS+, S2+, H+(OCS), and C2H5+ with OCS Molecules in the Gas Phase *J Am. Soc. Mass Spectrom.* **2005,** *16* (11), 1760–1771.
37. Pos, W. H.; Riener, D. D.; Zika, R. G., Carbonyl Sulfide OCS and Carbon Monoxide CO in Natural Waters: Evidence of a Coupled Production Pathway. *Marine Chemistry* **1998,** *62* (1-2), 89-101.
38. Stimler, K.; Montzka, S. A.; Berry, J. A.; Rudich, Y.; Yakir, D., Relationships Between Carbonyl Sulfide (COS) and CO2 During Leaf Gas Exchange. *New Phytologist* **2010,** *186* (4), 869-878.
39. Khalil, M. A. K.; Rasmussen, R. A., Global Sources, Lifetimes and Mass Balances of Carbonyl Sulfide (OCS) and Carbon Disulfide (CS2) in the Earth's Atmosphere. *Atmospheric Environment* **1984,** *18* (9), 1805-1813.

40. Ueno, Y.; Johnson, M. S.; Danielache, S. O.; Eskebjerg, C.; Pandey, A.; Yoshida, N., Geological Sulfur Isotopes indicate Elevated OCS in the Archean Atmosphere, Solving Faint Young sun paradox. *P.N.A.S.* **2009,** *106* (35), 14784-14789.
41. Cabaço, M. I.; Besnard, M.; Vaca-Chávez, F.; Pinaud, N.; Sebastião, P. J.; Coutinho, J. A. P.; Mascetti, J.; Danten, Y., On the chemical reactions of carbon dioxide isoelectronic molecules CS2 and OCS with 1-butyl-3-methylimidazolium acetate. *Chem. Commun.* **2013,** *49*, 11083-11085.
42. Cabaço, M. I.; Besnard, M.; Vaca-Chávez, F.; Pinaud, N.; Sebastião, P. J.; Coutinho, J. A. P.; Danten, Y., Understanding Chemical Reactions of CO_2 and its Isoelectronic Molecules with 1-butyl-3-methylimidazolium acetate by Changing the Nature of the Cation: The Case of CS_2 in 1-butyl-1-methylpyrrolidinium Acetate sStudied by NMR Spectroscopy and Density Functional Theory Calculations. *J. Chem. Phys.* **2014,** *140* (24), 244307.
43. Favier, I.; Castillo, A. B.; Godard, C.; Castilllon, S.; Claver, C.; Gomez, M.; Teuma, E., Efficient Recycling of a Chiral Palladium cCatalytic System for Asymmetric Allylic Substitutions in Ionic Liquid. *Chem. Commun.* **2011,** *47*, 7869-7871.
44. M. J. Frisch; G. W. Trucks; H. B. Schlegel; G. E. Scuseria; M. A. Robb; J. R. Cheeseman; G. Scalmani; V. Barone; B. Mennucci; G. A. Petersson, et al. *Gaussian 09*, Revision D.01; Gaussian Inc.: Wallingford CT 2009.
45. Sonnenberg, J. L.; Schlegel, H. B.; Hratchian, H. P., Spin Contamination in Inorganic Chemistry Calculation. In *Computational Inorganic and Bioinorganic Chemistry*, Solomon, E. I.; R.A.Scott; King, R. B., Eds. John Wiley & Sons 2009.
46. Jensen, F., *Introduction to Computational Chemistry* John Wiley & Sons: New York, 2007.
47. Chai, J. D.; Head-Gordon, M., Long-range Corrected Hybrid Density Functionals with Damped Atom-atom Dispersion Corrections. *Phys. Chem. Chem. Phys.* **2008,** *10*, 6615-6620.
48. Zhao, Y.; Trulhar, D. G., MQZVP Basis Set reference. *Theor. Chem. Account* **2008,** *120* 215-241.
49. Zhao, Y.; Truhlar, D. G., The M06 Suite of Density Functionals for Main Group Thermochemistry,Thermochemical Kinetics, Noncovalent Interactions, Excited states, and Transition Elements: Two New Functionals and Systematic Testing of Four M06-class Functionals and 12 Other Functionals. *Theor. Chem. Acc.* **2008,** *120*, 215-241.
50. Basiuk, V. A.; A.H.C.Escobar; Molina, H. M. M., Basis Set Effects on B3LYP Geometries and Energies: Case Study of Interstellar Reaction HN=CH2 + •C≡N ; H2N—C(•)H—C≡N. *Int. J. Quantum Chem.* **2002,** *87*, 101-109.
51. Arnaud, R.; C.Adamo; M.Cossi; A.Milet; Y.Vallée; V.Barone, Theoretical Study of the Addition of Hydrogen Cyanide to Methanimine in the Gas Phase and in Aqueous Solution. *J.Am. Chem. Soc.* **2000,** *122*, 324-330.
52. Voutchkova, A. M.; Feliz, M.; Clot, E.; Eisenstein, O.; Crabtree, R. H., Imidazolium Carboxylates as Versatile and Selective N-Heterocyclic Carbene Transfer Agents: Synthesis, Mechanism, and Applications. *J. Am. Chem. Soc.* **2007,** *129*, 12834-12846.
53. Ayala, P. Y.; Schlegel, H. B., A Combined Method for Determining Reation Paths, Minima and Transition State Geometries. *J.Chem. Phys.* **1997,** *107*, 375-384.
54. Peng, C.; Ayala, P. Y.; Schlegel, H. B.; Frisch, M. J., Using Redundant Internal Coordinates to Optimize Equilibrium Geometries and Transition States *J. Comp. Chem.* **1996,** *17* 49-56.
55. Peng, C.; Schlegel, H. B., Combining Synchronous Transit and Quasi-Newton Methods for Finding Transition States. *Israel J. Chem.* **1993,** *33* 449-54.
56. Hratchian, H. P.; Schlege**l,** H. B., Using Hessian Updating to Increase the Efficiency of a Hessian Based Predictor-corrector Reaction Path Following Method
J. Chem. Theo. and Comput. **2005,** *1*, 61-69.
57. Sarotti, A. M.; S.C.Pellegrinet, A multi-standard approach for GIAO (13)C NMR calculations. *J Org Chem.* **2009,** *74* (19), 7254-60.
58. Fulmer, G. R.; Miller, A. J. M.; Sherden, N. H.; Gottlieb, H. E.; Nudelman, A.; Stoltz, B. M.; Bercaw, J. E.; Goldberg, K. I., *Organometallics* **2010,** *29*, 2176.
59. Zsolt Kelemen; Barbara Péter-Szabo; Edit Székely; Oldamur Holloczki; Dzmitry S. Firaha; Barbara Kirchner; Jozsef Nagy; Nyulaszi, L., An Abnormal N-Heterocyclic Carbene–Carbon Dioxide Adduct from Imidazolium Acetate Ionic Liquids: The Importance of Basicity. *Chem. Eur. J* **2014,** *20*, 13002-13008.
60. Kuhn, N.; Bohnen, H.; Hankel, G., Zur reaktion von carben-addukten des kohlentoffdisulfides mit brom und iod. *Z. Naturforsch.* **1994,** *49b*, 1473-1480.

61. A.Moser; Range, K.; York, D., *J. Phys.Chem* **2010,** *114*, 13911-13921.
62. Linstrom, P.; Mallard, W., *NIST Standard Reference DataBase* NIST Chemistry WebBook ed.; 2003; Vol. 69.
63. Cabaço, M. I.; Besnard, M.; Danten, Y.; Coutinho, J. A. P., Solubility of CO2 in 1-Butyl-3-methyl-imidazolium-trifluoro Acetate 2 Ionic Liquid Studied by Raman Spectroscopy and DFT Investigations. *J Phys Chem B* **2011,** *115*, 3538-3550.

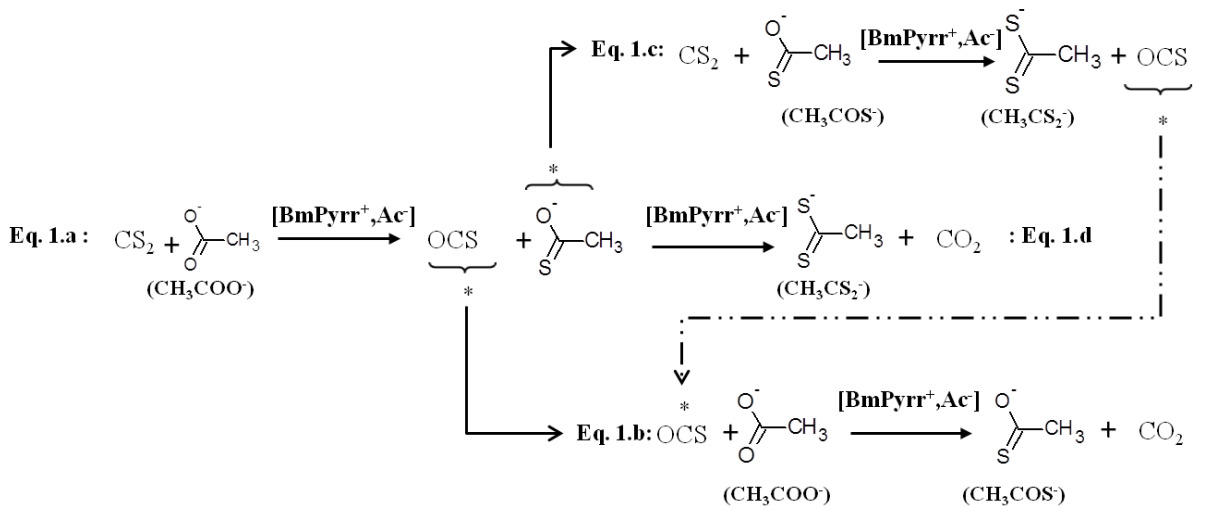

Scheme 1: Schematic representation of the main channels for the conversion mechanism of CS_2 into CO_2 with [BmPyrr][Ac] (Eqs. 1a, 1b) and of the secondary mechanisms due to the S-O exchange of the triatomic solutes CS_2 and OCS with thio-acetate anion (Eqs. 1c, 1d).

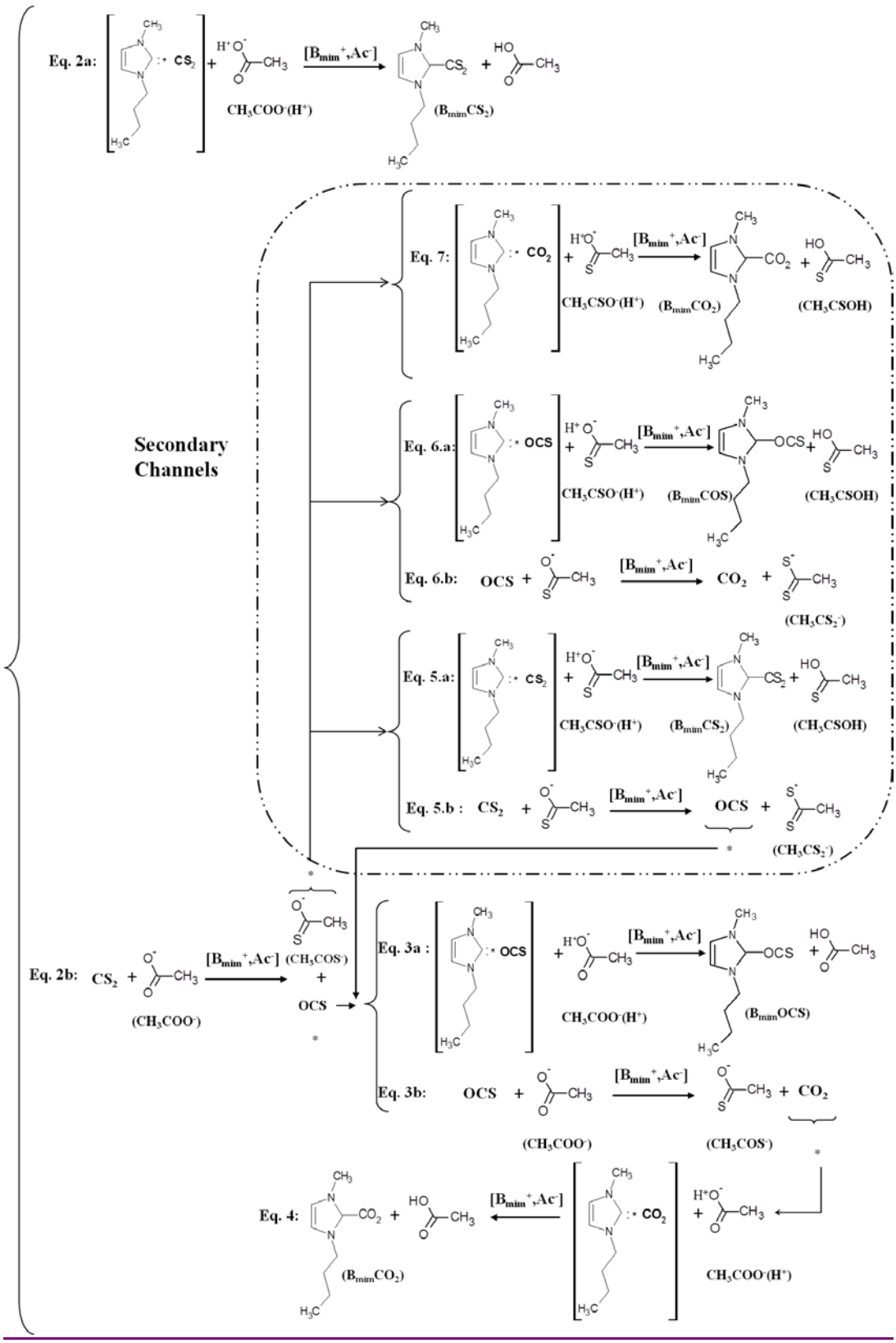

Scheme 2: Schematic representation of the competitive channels of reactions issued from the coexistence of the processes of capture of CS_2 (Eq.2.a) and of its degradation adducts by the imidazolium cation (Eq. 3a)with the degradation mechanisms of CS_2 into OCS (Eq. 2b) and of OCS into CO_2 (Eq. 3b). A separation in two distinct branches from a first conversion of CS_2 into OCS (Eq.2.b) discerns the secondary channels of reactions involving thioacetate anion in capture mechanisms (Eq. 5a and 6a) and degradation (Eqs. 5b, 6b). In this scheme, the spontaneous carboxylation from the formation of CO_2 is assumed as the ultimate reaction with the formation of imidazolium-2-carboxylate determining with the end point of the degradation cycle of CS_2 in imidazolium-acetate solutions. In contrast, the dithiocarboxylation reaction (Eq.2a) constitutes the unique reaction belonging to another independent branch of the scheme.

Table 1: ^{13}C NMR chemical shifts (ppm) for the C atoms (in bold) of the species in the initial and final structures (reactants/products) determined using the multi-standard analysis [57] for the calculated 'gas phase' pathways associated with the S-O exchanges processes for the solutes CS_2 and OCS interacting the N-butyl-N-methylpyrrolidinium acetate ion pair. The experimental values are displayed for comparison [42].

	Primary S-O exchange			Secondary S-O exchange		
	Eq. 1a	**Eq. 1b**		**Eq. 1d**	**Eq. 1c**	**Exp**
Atom in Species in	**Struct. 1.1**	**Struct. 1.2**		**Struct. 1.3**	**Struct. 1.4**	
CH3**C**OO$^-$	168.5	168.0				174.2
CS_2	195.2				195.2	193.0 [a]
O**C**S		150.4		150.0		159.0
CH3**C**OS$^-$				212.6	216.2	213.0
Atom in Species in	**Prd. 1.1**	**Prd. 1.2**		**Prd. 1.3**	**Prd. 1.4**	
CH3**C**OS$^-$	212.6	212.6				213.1
CS_2						
O**C**S	150.0				150.0	159.3
CO_2		118.5		118.2		125.0
CH3**C**SS$^-$				263.4	261.0	n.obs.

[a] ref [58].

Table 2: ^{13}C NMR chemical shifts (ppm) for the C atoms (in bold) of the species in the initial and final structures (reactants/products) determined using the multi-standard analysis [57] for the calculated 'gas phase' pathways associated with the capture of CS_2, OCS and CO_2 by imidazolium-ylidene-carbene ring (Eqs. 2a, 3a and 4, primary processes; Eqs. 5a, 6a and 7secondary processes) and with the S-O exchanges between acetate and the solutes CS_2 (Eqs. 2b, 5b) and OCS (Eqs. 3b, 6b) interacting the 1-butyl-3-methylimidazolium acetate ion pair. The experimental values are displayed for comparison [42].

	Eq. 2a	**Eq. 2b**	**Eq. 3a**	**Eq. 3b**	**Eq. 4**	**Eq. 5b**	**Eq. 5a**	**Eq. 6b**	**Eq. 6a**	**Eq. 7**	
C atom in species in	**Structure 1.1 (=Structure 1.2)**		**Structure 1.3 (=Structure 1.4)**		**Structure 1.5**	**Structure 1.6 (=Structure 1.8)**		**Structure 1.7 (=Structure 1.9)**		**Structure 1.10**	**Exp**
CH3**C**OO$^-$	171.1		169.7		169.5						175.0
CS_2	193.9					198.1					193 0[a]
C_2[Bmim]	146.6		146.8		146.0	140.2		140.1		140.2	139.0
O**C**S			150.4					150.5			156.0
CO_2					118.4					118.2	125.0
CH3**C**OS$^-$						215.6		216.4		217.2	213.0
C atom in species in	**Prd 1.1**	**Prd 1.2**	**Prd 1.3**	**Prd 1.4**	**Prd 1.5**	**Prd 1.6**	**Prd 1.8**	**Prd 1.7**	**Prd 1.9**	**Prd 1.10**	
Bmim**C**S_2	228.3						227.3			227.3	226-229
C_2 [BmimCS_2]	140.7						141.8			141.8	149 [b]
BmimO**C**S			203.4						183.1		192
C_2 [BmimOCS]			156.5						137.2		145
Bmim**C**O_2					146.4						155
C_2 [BmimCO_2]					139.0						142
CH3**C**OOH	164.7		184.5								[c]
CH3**C**SOH							216.2		217.6	216.2	
CH3**C**OS$^-$		215.0		216.3							215
C_2[Bmim]		141.0		141.5		144.1		143.5			139.0
CS_2											
O**C**S		149.7				150.2					156
CO_2				117.5				118.5			125.0
CH3**C**SS$^-$						263.1		263.5			n.obs.

[a] Ref [58]

[b] Refs. [6, 34, 60]. Not observed in [Bmim][Ac]-CS_2 solutions [42].

[c] The presence of the formed CH_3COOH was detected using the ^{1}H chemical shift [42].

Fig. Captions

Fig. 1: Calculated reaction paths associated with the mechanisms of conversion of CS_2 into OCS and OCS into CO_2 by interatomic S-O exchanges between solute and acetate anion in [BmPyrr][Ac] ion pair (Eqs. 1a and 1b, respectively, Scheme 1) calculated at the wB97xD/BS1 level (with $\Delta X(=E^{0+ZPE})$ ([BmPyrr][Ac]-OCS) is -12.2 kcal/mol, cf. Table S2). A schematic representation of the calculated energy minimum structures along these two predicted 'gas phase' pathways is also provided (schematic representation of all the anchored stationary points, energy minima and transition states calculated along both pathways is reported in the Supporting Information).

Fig. 2: E^{0+ZPE} energy diagrams associated with the mechanisms of conversion of CS_2 into OCS and OCS into CO_2 by interatomic S-O exchanges between solute and thioacetate anion in [BmPyrr][CH_3COS^-] ion pair (Eqs. 1c and 1d, respectively, Scheme 1) calculated at the wB97xD/BS1 level (with $\Delta X(=E^{0+ZPE})$([BmPyrr][CH_3COS^-]-CS_2) is -5.7 kcal/mol, cf. Table S4). The energy diagrams associated with these secondary mechanisms (red) are compared with those associated with the main conversion processes (blue) shown in Fig. 1.

Fig. 3: Calculated reaction paths associated with the mechanisms of capture of the solutes CS_2, OCS and CO_2 (Eqs. 2a, 3a and 4, respectively, Scheme 2) in [Bmim][Ac] ion pair and with the conversions of CS_2 into OCS and of OCS into CO_2 by interatomic S-O exchanges between solute and acetate anion (Eqs. 2b and 3b, respectively) calculated at the wB97xD/BS1 level (with $\Delta X(=E^{0+ZPE})$([Bmim][Ac]-OCS) and $\Delta X(=E^{0+ZPE})$([Bmim][Ac]-CO2) are -13.2 and -24.3 kcal/mol, cf. Table S5). A schematic representation of the calculated energy minimum structures along the predicted 'gas phase' pathways is also provided (more details are reported in the Supporting Information).

.

Fig. 4: E^{0+ZPE} energy diagrams associated with the secondary mechanisms of conversion of CS_2 into OCS (Eq. 5b, Scheme 2) and of OCS into CO_2 (Eq. 6b) in [Bmim][CH_3COS^-] ion pair and of capture of the solutes CS_2, OCS and CO_2 (Eqs. 5a, 6a and 7) calculated at the wB97xD/BS1 level ($\Delta X(=E^{0+ZPE})$([Bmim][CH_3COS^-]-CS2) and $\Delta X(=E^{0+ZPE})$([Bmim][CH_3COS^-]-CO2) are -6.4 and -15.3 kcal/mol, Table S6). The energy diagrams associated with these secondary mechanisms (red) are compared with those associated with the main processes (blue) shown in Fig. 3.

Fig. 1

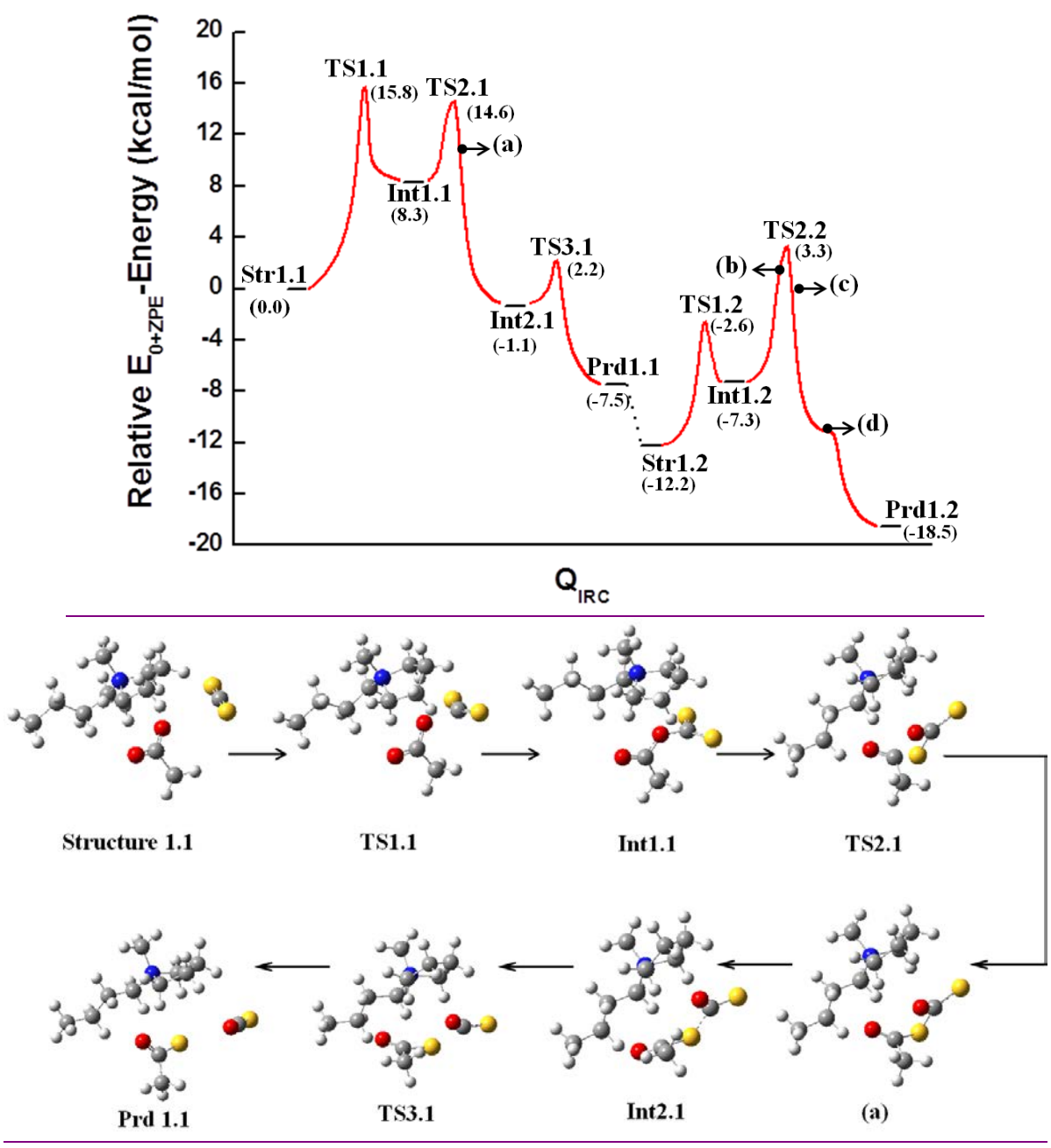
Relative E_{0+ZPE}-Energy (kcal/mol)
20
16
12
8
4
0
-4
-8
-12
-16
-20
TS1.1
(15.8)
TS2.1
(14.6)
(a)
Int1.1
(8.3)
Str1.1
(0.0)
TS3.1
(2.2)
Int2.1
(-1.1)
Prd1.1
(-7.5)
TS2.2
(3.3)
(b)
(c)
TS1.2
(-2.6)
Int1.2
(-7.3)
(d)
Str1.2
(-12.2)
Prd1.2
(-18.5)
Q_{IRC}
Structure 1.1
TS1.1
Int1.1
TS2.1
(a)
Int2.1
TS3.1
Prd 1.1

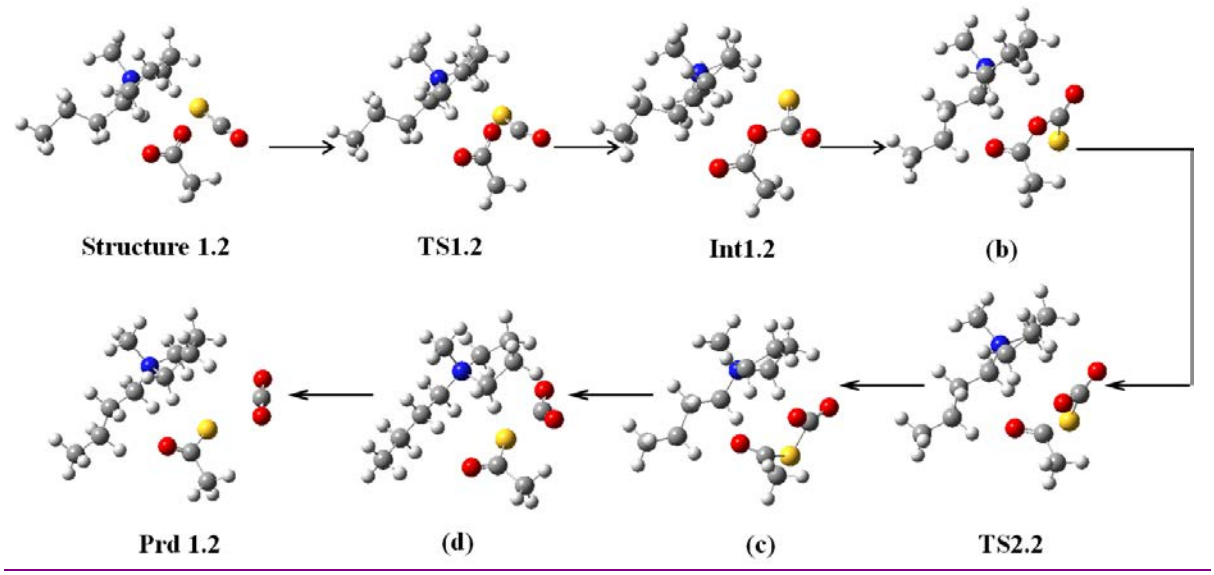
Structure 1.2
TS1.2
Int1.2
(b)
TS2.2
(c)
(d)
Prd 1.2

Fig. 2

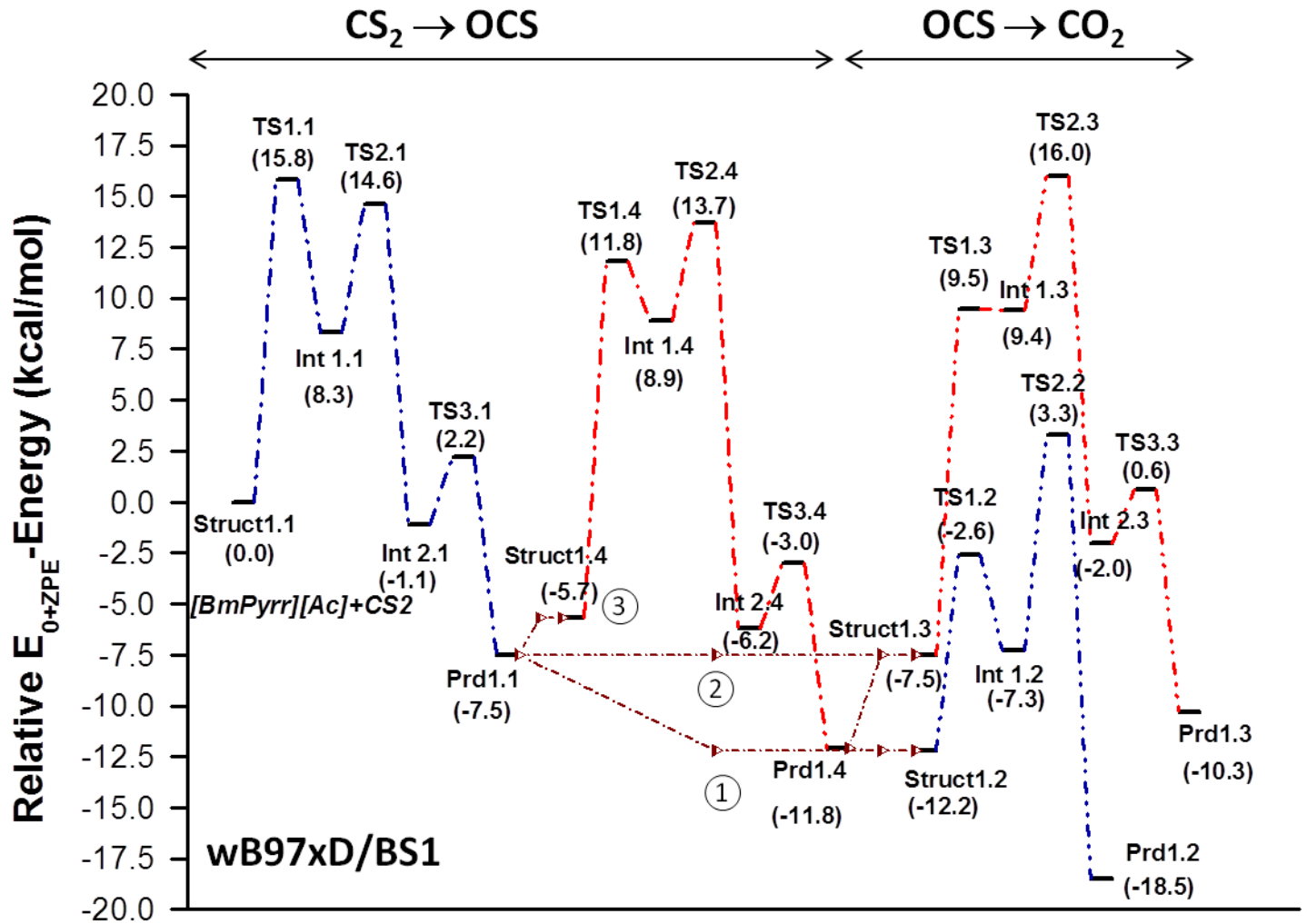
CS2 → OCS
OCS → CO2
Relative E0+ZPE-Energy (kcal/mol)
20.0
17.5
15.0
12.5
10.0
7.5
5.0
2.5
0.0
-2.5
-5.0
-7.5
-10.0
-12.5
-15.0
-17.5
-20.0
TS1.1 (15.8)
TS2.1 (14.6)
Int 1.1 (8.3)
TS3.1 (2.2)
Int 2.1 (-1.1)
Struct1.1 (0.0)
[BmPyrr][Ac]+CS2
TS1.4 (11.8)
TS2.4 (13.7)
Int 1.4 (8.9)
Struct1.4 (-5.7)
3
Int 2.4 (-6.2)
TS3.4 (-3.0)
Prd1.1 (-7.5)
2
1
Prd1.4 (-11.8)
Struct1.3 (-7.5)
TS1.3 (9.5)
Int 1.3 (9.4)
TS2.3 (16.0)
TS2.2 (3.3)
TS1.2 (-2.6)
Int 1.2 (-7.3)
Struct1.2 (-12.2)
TS3.3 (0.6)
Int 2.3 (-2.0)
Prd1.3 (-10.3)
Prd1.2 (-18.5)
wB97xD/BS1

Fig. 3

A)

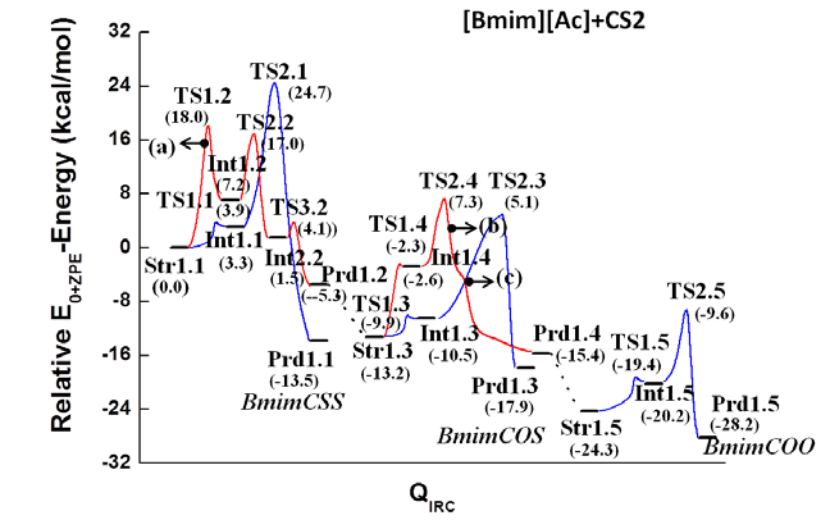
[Bmim][Ac]+CS2
Relative E0+ZPE-Energy (kcal/mol)
32
24
16
8
0
-8
-16
-24
-32
QIRC
Str1.1 (0.0)
TS1.1 (18.0)
Int1.1 (3.3)
TS2.1 (24.7)
Int2.1 (7.2)
TS3.2 (4.1)
Prd1.1 (-13.5)
BmimCSS
TS1.2 (3.9)
TS2.2 (17.0)
Int2.2 (1.5)
Prd1.2 (-5.3)
(a)
TS1.3 (-9.9)
Str1.3 (-13.2)
Int1.3 (-10.5)
TS2.3 (5.1)
TS2.4 (7.3)
TS1.4 (-2.3)
Int1.4 (-2.6)
(b)
(c)
Prd1.3 (-17.9)
BmimCOS
Prd1.4 (-15.4)
TS1.5 (-19.4)
Int1.5 (-20.2)
Str1.5 (-24.3)
TS2.5 (-9.6)
Prd1.5 (-28.2)
BmimCOO

B)

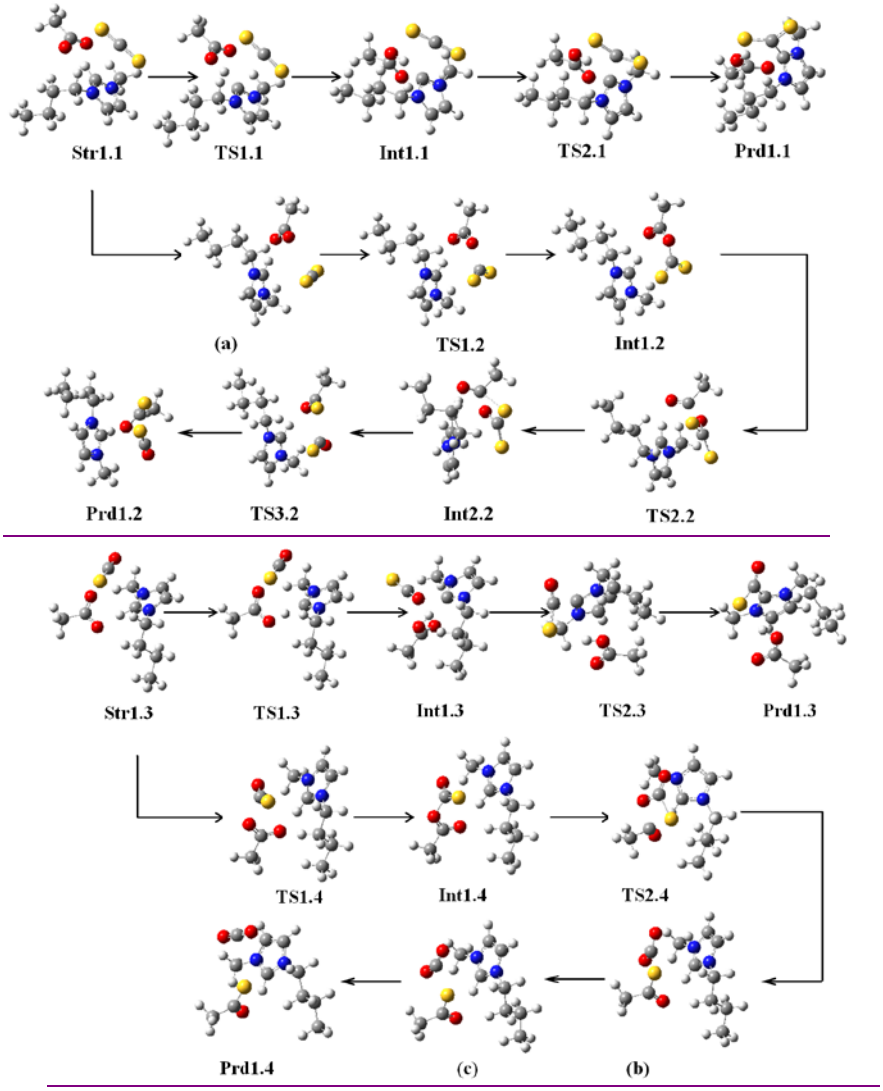
Str1.1
TS1.1
Int1.1
TS2.1
Prd1.1
(a)
TS1.2
Int1.2
Prd1.2
TS3.2
Int2.2
TS2.2
Str1.3
TS1.3
Int1.3
TS2.3
Prd1.3
TS1.4
Int1.4
TS2.4
Prd1.4
(c)
(b)

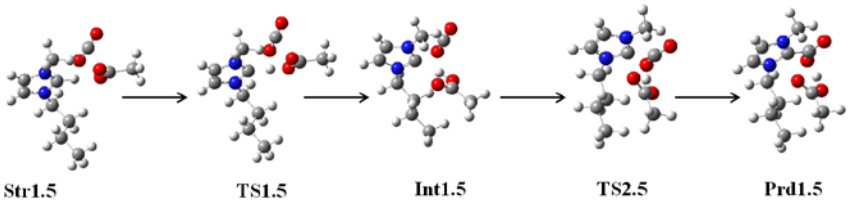
Str1.5
TS1.5
Int1.5
TS2.5
Prd1.5

Fig. 4

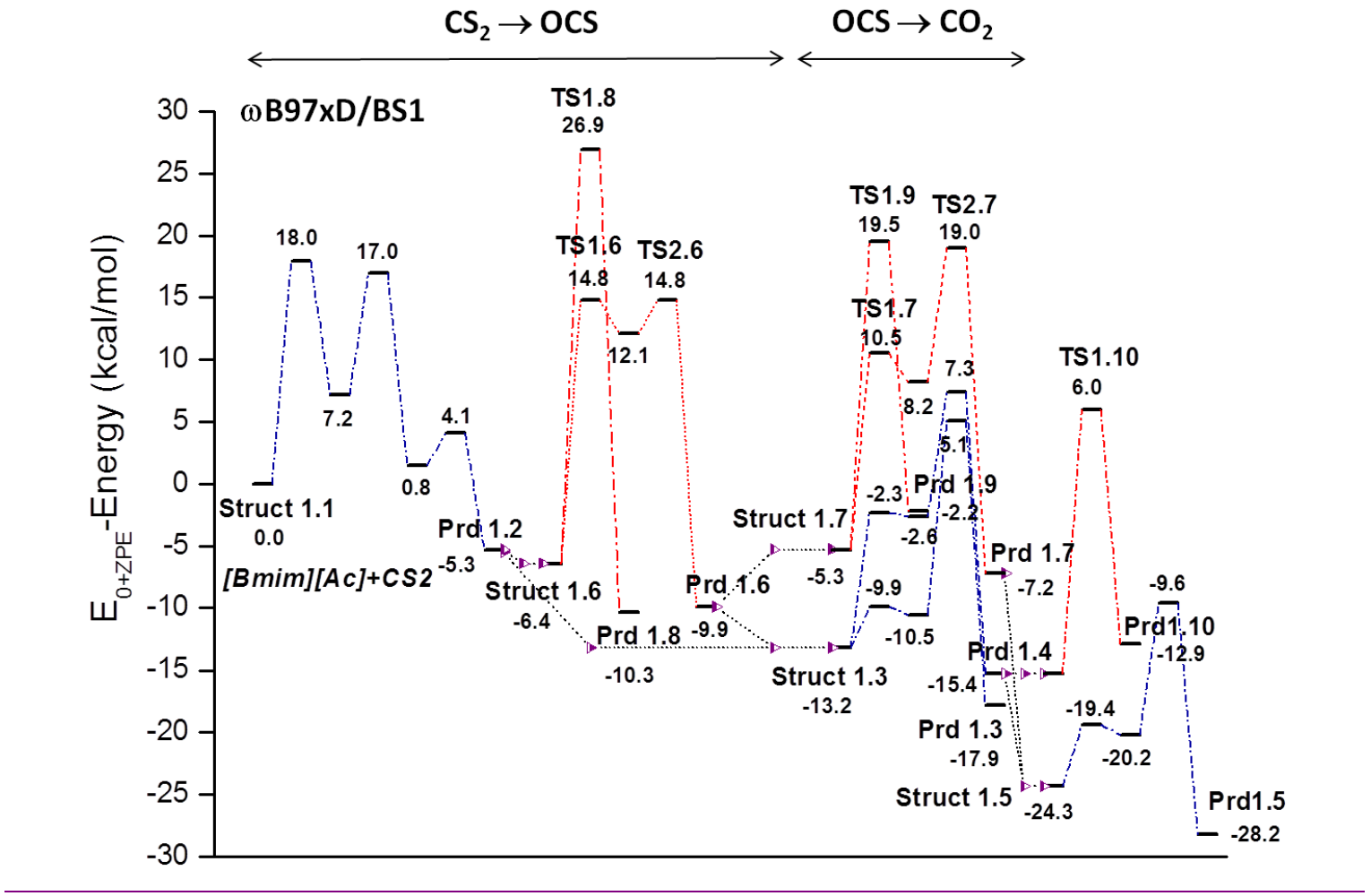
CS2 → OCS
OCS → CO2
ωB97xD/BS1
E0+ZPE-Energy (kcal/mol)
30
25
20
15
10
5
0
-5
-10
-15
-20
-25
-30
[Bmim][Ac]+CS2
Struct 1.1
0.0
18.0
7.2
17.0
0.8
4.1
Prd 1.2
-5.3
TS1.8
26.9
TS1.6
14.8
TS2.6
14.8
12.1
Struct 1.6
-6.4
Prd 1.8
-10.3
Prd 1.6
-9.9
Struct 1.7
-5.3
TS1.9
19.5
TS1.7
10.5
8.2
-2.3
-2.6
Prd 1.9
-2.2
TS2.7
19.0
7.3
5.1
-9.9
-10.5
Struct 1.3
-13.2
Prd 1.7
-7.2
TS1.10
6.0
Prd 1.4
-15.4
Prd 1.3
-17.9
Struct 1.5
-24.3
-19.4
-20.2
-9.6
Prd1.10
-12.9
Prd1.5
-28.2

Table of Contents Graphic: